Effects of Linear Perspective on Human Use of Preview in Manual Control

van der El, Kasper; Pool, Daan M.; van Paassen, Marinus M.; Mulder, Max

DOI
10.1109/THMS.2017.2736882

Publication date
2018

Document Version
Accepted author manuscript

Published in
IEEE Transactions on Human-Machine Systems

Effects of Linear Perspective on Human Use of Preview in Manual Control

Kasper van der El, *Student Member, IEEE,* Daan M. Pool, *Member, IEEE,*
Marinus (René) M. van Paassen, *Senior Member, IEEE,* and Max Mulder

***Abstract*—Due to linear perspective, the visual stimulus provided by a previewed reference trajectory reduces with increasing distance ahead. This paper investigates the effects of linear perspective on human use of preview in manual control tasks. Results of a human-in-the-loop tracking experiment are presented, where the linear perspective's horizontal and vertical deformation along the previewed trajectory were applied separately and combined, or were absent (plan-view task). Measurements are analyzed with both nonparametric and parametric system identification techniques, in combination with a quasi-linear human controller model for plan-view preview tracking tasks. Results show that reduced visual stimuli in perspective tasks evoke less aggressive control behavior, but that the human's underlying control mechanisms are still accurately captured by the model. We conclude that human controllers use preview information similar in plan-view and perspective tasks.**

***Index Terms*—Linear perspective, man-machine systems, manual control, parameter estimation, preview, system identification**

I. Introduction

HUMANS rely heavily on visual information in many manual control tasks. An important visual cue is preview, information about the future reference trajectory, or target, to follow. Examples of preview include the road ahead when driving [1]–[3] or cycling [4], and an artificially displayed tunnel-in-the-sky when piloting a helicopter [5] or aircraft [6]. Preview enables humans to apply feedforward control to anticipate upcoming trajectory changes [7].

To study the human controller's (HC) use of preview information, simplified tracking tasks are often performed with a plan-view (i.e., two-dimensional or top down) display [8]–[12]. Removal of all other control-related cues, like physical motion and optic flow, then allows for explicit measuring and identification of the HC's response to preview information. Recent modeling efforts [11] and subsequent analysis [12] suggested that HCs apply a dual-mode control strategy: open-loop control based on a point on the target close ahead, the "near" viewpoint, and closed-loop control based on a point farther ahead, the "far" viewpoint.

The novel preview model from [11] extends McRuer *et al.*'s [13], [14] famous crossover model for compensatory tracking; as such, it may facilitate a similar structured, quantitative approach to design and evaluate human-machine systems (e.g., interfaces), but for more realistic control tasks. However, general vehicle control tasks differ markedly from the preview tracking experiments in [8]–[12], as the target trajectory is often viewed from a point within the visual scene, like a camera on a remote vehicle or the human eye. First, due to linear perspective, the previewed target trajectory appears increasingly compressed with distance ahead, while the target in the plan-view tracking experiments is displayed equally large nearby and far ahead. Second, the visual flow field provides additional cues of the viewpoint's rotations and translations [15], [16]. The HC's excellent adaptive capabilities [13], [17] make it difficult to predict if and how these two factors affect HC behavior.

In this paper, we focus on the effects of linear perspective, because the reducing visual stimuli from the target farther ahead, and the corresponding magnification of parts nearby, may severely affect the near- and far-viewpoint responses adopted by the HC. On the one hand, it was shown in compensatory tracking tasks that smaller visual stimuli evoke less aggressive control behavior and larger response time-delays [18], [19]. This would suggest that the HC's response to preview far ahead, which is strongly affected by perspective, will be weaker in perspective tasks (compared to plan-view tasks). On the other hand, perception research has shown that the human's visual system compensates visual stimuli with simultaneously sensed depth cues [20]; as such, HC perception (and hence control) of a previewed target might still be equal in plan-view and perspective tasks.

Perspective displays have been extensively studied, and applied, as they allow for intuitive three-dimensional spatial information transfer (e.g., see [21]–[23]). Unfortunately, these studies did not measure – and thus did not increase our understanding of – the HC's underlying control behavior. The HC's control dynamics were measured in other perspective control tasks, like driving and flying, but these tasks lacked preview information [18], [24], or did not explicitly reveal the effects of linear perspective on the HC's near- and far-viewpoint responses [1], [2], [4], [6], [25].

The goal of this paper is to explicitly quantify how linear perspective affects HC use of preview information, and specifically the near- and far-viewpoint response mechanisms. Measurements from a human-in-the-loop experiment are analyzed, in which eight subjects performed a tracking task with integrator controlled element (CE) dynamics, and 2 s of preview. The preview was shown either in plan-view, or with the horizontal and vertical perspective deformations along the previewed trajectory applied separately, as well as combined. First, objective measures are calculated to quantify tracking performance, control activity, and coherence. Next, a non-

The authors are with the Control and Simulation section, Faculty of Aerospace Engineering, Delft University of Technology, 2629 HS Delft, The Netherlands. Corresponding author: k.vanderel@tudelft.nl

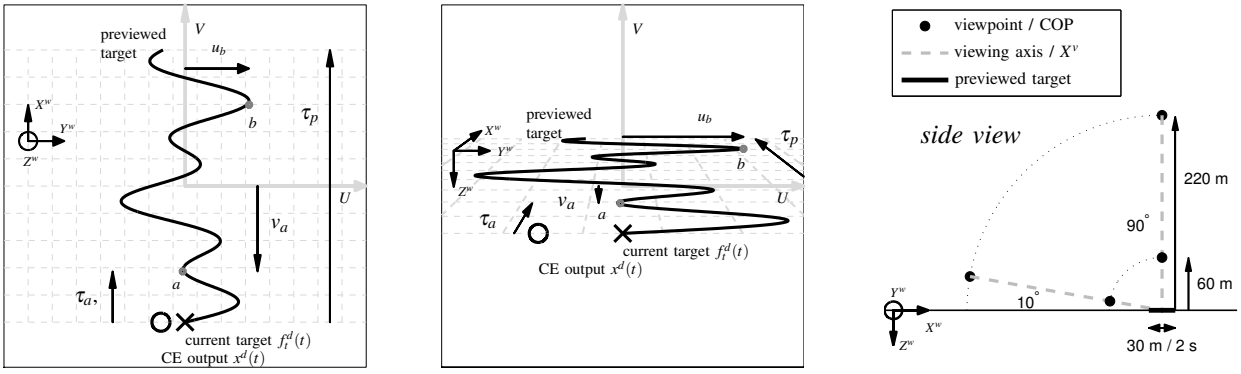

Fig. 1. Plan-view (a) and perspective (b) preview displays, obtained by viewing the target from points "90°/220 m" and "10°/60 m", respectively (c).

parametric, multiloop, frequency-domain system identification method is applied [26], and the parameters of the HC model for plan-view preview tracking tasks from [11] are estimated. The obtained HC dynamics and model parameters explicitly characterize how HCs adapt their control behavior between plan-view and perspective tasks.

This paper is structured as follows. In Section II we introduce the preview control task and linear perspective. In Sections III and IV we elaborate on our methods: the HC model for plan-view preview tracking tasks from [11], the applied system identification techniques, and the performed experiment. Results are presented in Section V, followed by a discussion and our main conclusions in the final two sections.

II. Preview Tracking and Linear Perspective

A. The Control Task

In this paper, we consider a single-axis, lateral position tracking task. The HC is required to minimize the lateral tracking error $e(t)$, which is the difference between the target signal $f_t(t)$ and the CE output $x(t)$:

$$e(t) = f_t(t) - x(t), \tag{1}$$

at current time t. The HC gives control inputs $u(t)$ to the CE, which is simultaneously perturbed by a disturbance signal $f_d(t)$. The task, illustrated in Figs. 1 and 2, is thus two-fold: target tracking and disturbance rejection.

In preview tracking tasks, the target ahead $f_t([t,t+\tau_p])$ is visible up to preview time τ_p. A plan-view of the previewed target is shown in Fig. 1a; this view corresponds to looking straight down from a point high above the previewed target (i.e., 90° elevation in Fig. 1c). Due to the viewpoint's movement parallel to world frame axis X^w, the previewed target moves down over the screen and forces the current target (cross) left and right. Note that, in a forced-pace (fixed velocity) task as we consider, time and distance are linearly related, so all signals can be written with time as the independent variable without loss of generality.

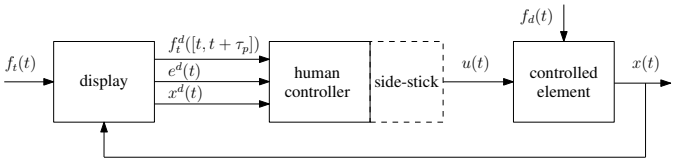

Fig. 2. The HC in a target-tracking and disturbance-rejection task.

The same scene observed from 10° elevation yields a perspective view (see Fig. 1b). Viewed from this particular point, the displayed target trajectory is compressed in vertical display direction V and magnified in horizontal display direction U. Vertical display coordinate v_a is much smaller on the perspective display than on the plan-view display, for the same point a on the previewed target τ_a s ahead. Horizontally, the display coordinate u_b is larger on the perspective display for any arbitrary point b on the previewed target. Clearly, the displayed signals (f_t^d, e^d, and x^d in Fig. 2), hence the visual stimuli from the previewed target, are markedly different in plan-view and perspective tasks.

B. Perspective Projection Method

Central projection is a technique to map a three-dimensional visual scene to a two-dimensional display surface [27]. The basic principle is similar to that of a camera, which produces a picture (i.e., a two-dimensional representation) of a three-dimensional visual scene. The center of projection (COP), or viewpoint, is the location from which the visual scene is supposedly observed (see Fig. 3). Light rays, or projectors, emanate from each point in the visual scene to converge in the COP. When a certain viewplane is defined at finite distance κ from the COP, the intersection of passing light-rays with this viewplane yields a two-dimensional image: the perspective projection. Alternatively, when κ is infinite, a parallel projection is obtained, yielding a plan-view. The COP is the origin of the view reference frame (superscript v), with the central viewing axis X^v defining the viewing direction. The boundaries of the visualized volume are characterized by the horizontal and vertical field of view (FOV):

$$\text{HFOV} = 2\arctan\left(\frac{w}{2\kappa}\right), \quad \text{VFOV} = 2\arctan\left(\frac{h}{2\kappa}\right), \tag{2}$$

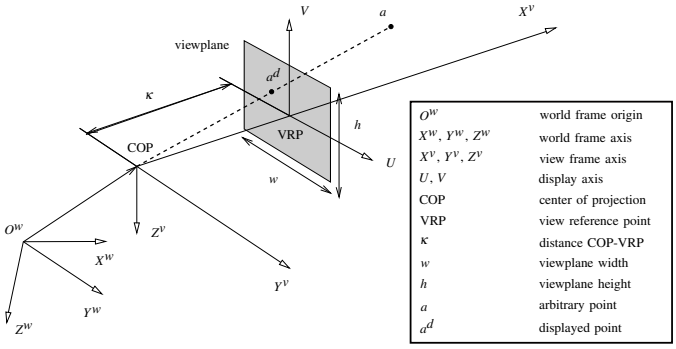

Fig. 3. The perspective projection method and its principal terminology.

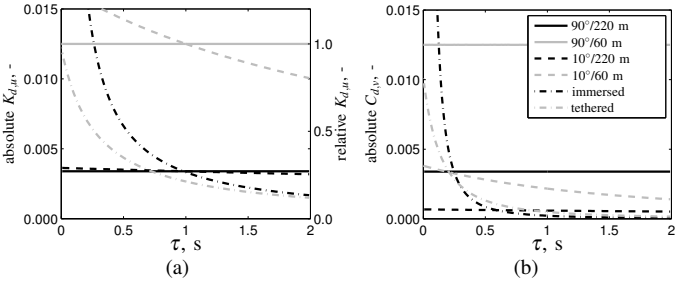

Fig. 4. Horizontal (a) and vertical (b) display scaling gains for various viewpoints, as a function of time τ along the previewed trajectory ahead.

with w and h the viewplane's width and height, respectively. For an arbitrary point a in the visual scene, the corresponding viewplane coordinates u_a and v_a are obtained from:

$$u_a = \kappa \frac{y_a^v}{x_a^v}, \qquad v_a = -\kappa \frac{z_a^v}{x_a^v}, \tag{3}$$

with x_a^v, y_a^v and z_a^v the coordinates of point a in the view reference frame.

C. Perspective Display Gains

HC task performance depends on the appearance of a perspective scene, as demonstrated by Kim *et al.* [21] for three-axis pursuit tracking tasks. It is possible to use the perspective projection's parameters (like FOV and elevation) to compare the appearances of perspective scenes; however, when analyzing HC behavior, it is more convenient to express perspective deformations as display scaling gains, as a function of time τ along the previewed trajectory ahead. In horizontal display direction, we define display gain $K_{d,u}(\tau)$ as the ratio of the display and world coordinates of an arbitrary point a in the visual scene:

$$K_{d,u}(\tau) = \frac{u_a(\tau)}{y_a^w(\tau)}. \tag{4}$$

In vertical display direction, we define gain $C_{d,v}(\tau)$ as the ratio of the displayed and real (i.e., in world coordinates) lengths of an element with length $d\tau$ as:

$$C_{d,v}(\tau) = \frac{v_a(\tau + d\tau) - v_a(\tau)}{y_a^w(\tau + d\tau) - y_a^w(\tau)}. \tag{5}$$

Notations K and C are adopted to emphasize the task's controlled and non-controlled directions: HCs can only control the CE laterally, so in horizontal display direction.

As an example, consider the situation in Fig. 1c: a target trajectory is visible for 30 m ahead, corresponding to 2 s of preview at a velocity of 15 m/s. Fig. 4 shows the display gains for all four COP's, for a κ of 75 cm. Looking straight down from 220 m height, each point on the previewed target is approximately equally far away from the COP, yielding a near-uniform scaling in both horizontal and vertical display directions with a ratio of 1:κ/220, or 1:0.0035 (black solid lines in Fig. 4). This projects the 30 m of preview to about 10 cm on the display, which corresponds roughly to the plan-view preview tracking task in [11] and [12]. Fig. 4 shows that a smaller object distance (i.e., moving the COP down vertically) yields higher display gains in both directions (gray solid line). For large object distances this magnification is nearly uniform, as all points of the previewed target remain approximately equally far from the COP.

Viewed from a non-vertical elevation, the object distance to the nearer part of the previewed target (small τ) is smaller than that of far parts (large τ). Therefore, the horizontal and vertical display gains will be larger for near points compared to far points, as illustrated for an elevation angle of 10° in Fig. 4 (black and gray dashed lines). This effect is more pronounced when the COP is closer to the previewed target, because the relative difference in object distance between near and far parts increases.

Fig. 4 also shows the display gains for an immersed and a tethered viewpoint, for a κ of 5 cm. The immersed viewpoint corresponds to a view from a car or bicycle, at 1 m height above the start of the previewed target (at τ=0 s), yielding display gains that are a strong nonlinear function of τ (black dash-dotted line). The display gains increase asymptotically to infinity for points close ahead (small τ), as these parts are outside the (forward aimed) viewing volume. A tethered viewpoint located 3.5 m above and behind the start of the previewed target yields similar display gains, but with the near points still in sight (gray dash-dotted line). Our experiment will include the display gains from this tethered view. For comparison, the right axis in Fig. 4a shows the horizontal display gains relative to that of the tethered view at τ=0 s.

III. Human Controller Modeling and System Identification

To investigate how linear perspective affects HC use of preview information, we analyze the experimental data with system identification techniques, in combination with a quasi-linear cybernetic model. This approach is explained here.

A. HC Model for Plan-view Preview Tracking Tasks

The HC model for plan-view preview tracking tasks from [11] is shown in Fig. 5, together with a display model. The display gains $K_{d,u}(\tau)$ scale the previewed target horizontally at the indicated time τ ahead. The relative display gains are used, such that the CE output $x(t)$ (located at τ=0 s) has unity scaling, as $K_{d,u}(0)$=1. It is mathematically equivalent to

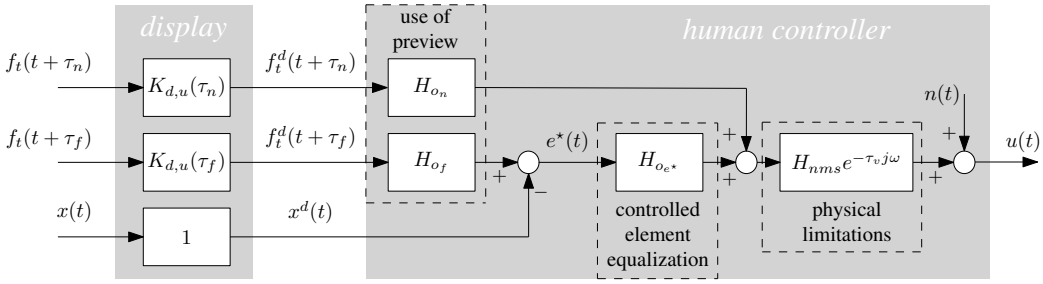

Fig. 5. Control diagram of the HC model for preview tracking tasks, adapted from [11] and augmented with a simple display model.

use the absolute display gains from Fig. 4, but this changes the interpretation of the gains in the HC model and makes comparisons with previous work less straightforward.

The HC model extends McRuer *et al.*'s [13], [14] crossover model for compensatory tracking tasks, with two viewpoints on the previewed target as inputs. It was found that this two-viewpoint model structure is sufficient to account for the HC's total response to a previewed target [11], [12]. A far-viewpoint $f_t(t+\tau_f)$ is the input to a feedback model for compensatory control behavior (similar as in the model by Modjtahedzadeh & Hess [28]), while a near-viewpoint $f_t(t+\tau_n)$ is the input to a parallel, additive open-loop response. The near- and far-viewpoints are located τ_n and τ_f s ahead on the previewed target, respectively. The model is quasi-linear, so linear functions describe most of the HC's behavior. Neither nonlinear and time-varying behavior, nor perception and motor noise are explicitly modeled; these are injected together as filtered white noise through the remnant $n(t)$.

Central to the model is the feedback response to an internal error $e^\star(t)$: a hypothetical, cognitively calculated signal, which cannot be measured. Fig. 5 shows that $e^\star(t)$ is the difference between the target in the far viewpoint, low-pass filtered by $H_{o_f}(j\omega)$, and the CE output:

$$E^\star(j\omega) = H_{o_f}(j\omega)F_t^d(\tau_f, j\omega) - X^d(j\omega). \tag{6}$$

The signals written in capitals denote the Fourier transform of the respective time domain signals, and $H_{o_f}(j\omega)$ is the following low-pass filter:

$$H_{o_f}(j\omega) = K_f \frac{1}{1+T_{l,f}j\omega}. \tag{7}$$

The time constant $T_{l,f}$ characterizes the bandwidth of the far-viewpoint response. It models the HC's cognitive elimination of the target signal's high frequencies from the far-viewpoint response, facilitated by the preview [12]. Gain K_f reflects the HC's ability to respond relatively more aggressive to the target (K_f>1) or to the CE output (K_f<1). When K_f=1 and $T_{l,f}$=τ_f=0 s, (6) and (7) show that $e^\star(t) = e(t)$, so that the HC responds to the real error.

The internal error response $H_{o_{e^\star}}(j\omega)$ is identical to McRuer *et al.*'s [14] simplified precision model:

$$H_{o_{e^\star}}(j\omega) = K_{e^\star}\frac{1+T_{L,e^\star}j\omega}{1+T_{l,e^\star}j\omega}, \tag{8}$$

with $K_{e^\star}$ the error response gain, and $T_{L,e^\star}$ and $T_{l,e^\star}$ the lead and lag equalization time constants, respectively. In compensatory tracking tasks, humans apply only proportional control when the CE has integrator dynamics [13] (as considered in this paper); however, estimated human control dynamics in preview tasks point to some low-frequency lag-lead equalization [11], [12].

At the target signal's high frequencies the far-viewpoint response is attenuated by the low-pass filter in $H_{o_f}(j\omega)$. Here, HCs predominantly apply open-loop control, which is captured in the model by the near-viewpoint response $H_{o_n}(j\omega)$. A gain K_n with a differentiator generally suffices to describe these control dynamics [12]:

$$H_{o_n}(j\omega) = K_n j\omega. \tag{9}$$

A near-viewpoint response is not always clearly present in preview tasks, and some HCs do not apply this control mechanism at all [11], [12].

The model also includes the HC's main physical limitations. Visual response time-delay τ_v combines perceptual, cognitive and transport delays, while $H_{nms}(j\omega)$ represents the combined side-stick and HC neuromuscular system (NMS) dynamics [29]:

$$H_{nms}(j\omega) = \frac{\omega_{nms}^2}{(j\omega)^2 + 2\zeta_{nms}\omega_{nms}j\omega + \omega_{nms}^2}, \tag{10}$$

with ω_{nms} and ζ_{nms} the natural frequency and damping ratio.

B. Nonparametric System Identification

The HC dynamics can be objectively estimated without making any assumptions, besides the model's inputs and outputs, using a nonparametric system identification method based on Fourier coefficients [26]. The resulting estimates, called describing functions, can validate the parametric model structure from the previous section.

1) Forcing Functions: Nonparametric system identification allows for the estimation of an equal number of describing functions as there are uncorrelated external inputs, called forcing functions [30]. To closely resemble common control tasks, only two forcing functions can be inserted in the considered preview tracking task: a target and a disturbance. By choosing multisine forcing functions (here with 20 sines each) high signal-to-noise ratio's are obtained at the input frequencies:

$$f_t(t) = \sum_{i=1}^{20} A_t[i]\sin(\omega_t[i]t + \phi_t[i]), \tag{11}$$

$$f_d(t) = \sum_{i=1}^{20} A_d[i]\sin(\omega_d[i]t + \phi_d[i]), \tag{12}$$

with amplitude $A[i]$, frequency $\omega[i]$ and phase $\phi[i]$ of the i^{th} sinusoid (see Section IV for the values used in the experiment). Selecting different input frequencies for the target and disturbance is sufficient for these two signals to be uncorrelated.

2) Model Restructuring: The two forcing functions allow for the identification of only two describing functions, so the model in Fig. 5 must first be converted to a two-channel model. The structure in Fig. 6 is convenient, as it separates the target-to-control dynamics $H^u_{f_t}(j\omega)$ from the CE-output-to-control dynamics $H^u_x(j\omega)$ [11], [12]. These dynamics can be expressed in terms of the HC dynamics and the display gains using block diagram algebra (for details, see [11]):

$$H^u_{f_t}(j\omega) = \big[K_{d,u}(\tau_f)H_{o_f}(j\omega)H_{o_{e^\star}}(j\omega)e^{\tau_f j\omega} + K_{d,u}(\tau_n)H_{o_n}(j\omega)e^{\tau_n j\omega}\big]H_{nms}(j\omega)e^{-\tau_v j\omega}, \quad (13)$$

$$H^u_x(j\omega) = H_{o_{e^\star}}(j\omega)H_{nms}(j\omega)e^{-\tau_v j\omega}. \quad (14)$$

Note that the HC dynamics and the display gains must be lumped in (13) and (14), as the visual stimulus provided by the perspectively transformed, displayed target f_t^d is unsuitable for linear frequency-domain analysis. The HC and display gains in (13) can be lumped together into effective gains:

$$K_{n,eff} = K_{d,u}(\tau_n)K_n, \qquad K_{f,eff} = K_{d,u}(\tau_f)K_f, \quad (15)$$

to easily compare results from plan-view and perspective tasks.

3) Multiloop Describing Function Estimation: Using Fig. 6, the control output can be written as:

$$U(j\omega) = H^u_{f_t}(j\omega)F_t(j\omega) - H^u_x(j\omega)X(j\omega) + N(j\omega). \quad (16)$$

A second equation is required to solve for the two unknown describing functions. Evaluating (16) only at the target signal input frequencies ω_t, a second equation can be obtained by interpolating the measured signals (U, F_t, X) in the frequency domain from the disturbance input frequencies ω_d to these same ω_t (indicated by $\tilde{U}$, $\tilde{F}_t$, $\tilde{X}$). Neglecting the remnant, which is small compared to the HC's response to the forcing functions at the input frequencies, it follows that [11], [26]:

$$\begin{bmatrix} U(j\omega_t) \\ \tilde{U}(j\omega_t) \end{bmatrix} = \begin{bmatrix} F_t(j\omega_t) & -X(j\omega_t) \\ \tilde{F}_t(j\omega_t) & -\tilde{X}(j\omega_t) \end{bmatrix} \begin{bmatrix} H^u_{f_t}(j\omega_t) \\ H^u_x(j\omega_t) \end{bmatrix}. \quad (17)$$

Solving (17) for $H^u_{f_t}(j\omega_t)$ and $H^u_x(j\omega_t)$ yields the describing function estimates at ω_t. Replacing ω_t by ω_d in (17), and interpolating all signals from ω_t to ω_d, yields the describing functions at ω_d. The method's complete derivation was published in [11], [26], [30]; examples of successful identification of HC behavior are found in [11], [12], [16], [30].

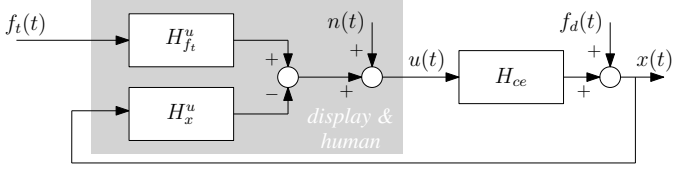

Fig. 6. Two-channel model used for system identification purposes; the display and HC models are lumped.

C. Parameter Estimation and Model Fitness

1) Parameter Estimation: The HC model's parameters can be estimated in the frequency domain by minimizing a criterion J that is based on the difference between the measured and the modeled control outputs [12]:

$$J(\hat{\Theta}) = \sum_{l=1}^{N_l} |U(j\omega_l) - \hat{U}(j\omega_l|\Theta)|^2. \quad (18)$$

The modeled output $\hat{U}(j\omega_l|\Theta)$ is given by (16) with remnant N=0; the model parameter vector Θ is $[K_{f,eff}\ \ \tau_f\ \ T_{l,f}\ \ K_{n,eff}\ \ \tau_n\ \ K_{e^\star}\ \ T_{L,e^\star}\ \ T_{l,e^\star}\ \ \tau_v\ \ \omega_{nms}\ \ \zeta_{nms}]^T$. N_l is the number of measured frequencies below a chosen cut-off frequency, here 25 rad/s. A Nelder-Mead simplex algorithm is often used to minimize J, constrained only to avoid solutions with negative parameters. Selecting the best solution from many randomly initialized optimizations (here we use 100) yields a high chance to find the global minimum. In a second step, the display gains $K_{d,u}(\tau)$ can be calculated at the estimated τ_n and τ_f, which can then be used to calculate the HC gains K_n and K_f with (15).

2) Variance Accounted For (VAF): The VAF is a measure for the similarity of two signals; its maximum, 100%, indicates that two signals are equal. When applied to compare the measured and the modeled control output the VAF inherently quantifies the model's ability to describe the measured HC behavior [31]. Because a signal's variance is equal to its integrated power-spectral density, the VAF can be calculated as follows:

$$\mathrm{VAF} = \left(1 - \frac{\sum_{l=0}^{N_s-1} P_{\varepsilon_u\varepsilon_u}(l\omega_b)}{\sum_{l=0}^{N_s-1} P_{uu}(l\omega_b)}\right) \times 100\%, \quad (19)$$

with N_s the number of samples in the measured time-traces and ω_b the fundamental radial frequency. P is the estimated periodogram of the subscripted signals, and ε_u is the difference between the measured and modeled control outputs:

$$\varepsilon_u(j\omega) = U(j\omega) - \hat{U}(j\omega|\Theta). \quad (20)$$

3) Coherence: The coherence is a measure for the linear relationship between two signals. A high coherence between the external input signals and the HC's control output can justify using a quasi-linear HC model to analyze the experimental data [31]. The value of the coherence is always between 0 (no linear relation) and 1 (perfect linear relation). The coherence $\Gamma_{f_t u}$ between the target signal and the control output is given by:

$$\Gamma_{f_t u}(\tilde{\omega}_t) = \sqrt{\frac{|\tilde{P}_{f_t u}(\tilde{\omega}_t)|^2}{\tilde{P}_{f_t f_t}(\tilde{\omega}_t)\tilde{P}_{uu}(\tilde{\omega}_t)}}, \quad (21)$$

The tilde indicates the average periodogram between the neighboring frequencies in a double band of input frequencies [31]. The coherence between the disturbance input signal and the HC output is calculated similarly.

IV. The Experiment

A. Independent Variables

The experiment had two independent variables, namely horizontal and vertical display scaling. Each had two levels: constant (plan-view) and perspective scaling. This design allows to investigate the difference in HC behavior between plan-view and perspective tasks, while separating the individual effects of horizontal and vertical perspective deformations. The full factorial of the two independent variables was tested, yielding four conditions: 1) constant scaling, or no perspective (NP), 2) horizontal perspective with constant vertical scaling (HP), 3) vertical perspective with constant horizontal scaling (VP), and 4) horizontal and vertical perspective combined (HVP).

The applied perspective scaling was in accordance with the tethered view in Fig. 4, so the entire previewed target was visible on the display. The plan-view's vertical scale was set to 5.08 cm/s of preview, which was similar as in [11] and [12], and corresponds to the "90°/220 m" condition in Fig. 4. The plan-view had unity horizontal scaling, equal to the tethered view at τ=0 s (see Fig. 4), yielding an equally large displayed error $e^d(t)$ in all four conditions; thereby, any measured changes in control behavior must be due to linear perspective. Pictures of all four displays are shown in Fig. 7, video's that further illustrate the conditions are available at http://ieeexplore.ieee.org.

B. Control Variables

1) Controlled Element: The CE had integrator dynamics, $H_{ce}(j\omega)=1.5/s$, with its gain of 1.5 tuned such that the operator could give accurate inputs, but would not reach the stick deflection limits during a normal run.

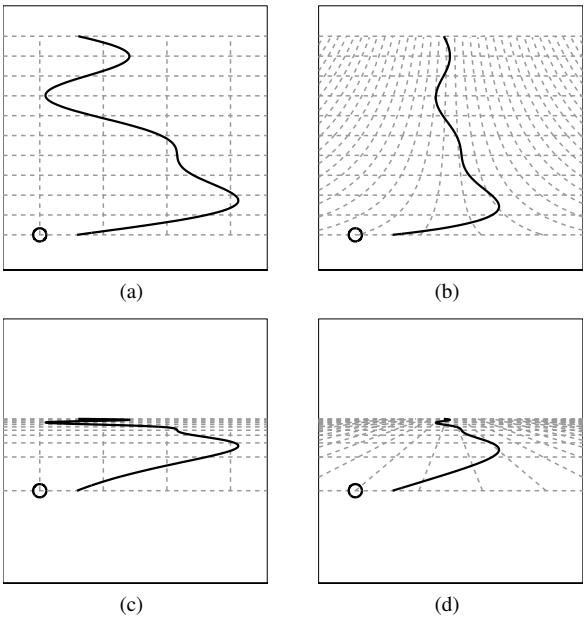

Fig. 7. Layout of the four experimental displays: NP (a), HP (b), VP (c), and HVP (d); the grid was not visible during the experiment.

2) Display: The display showed the previewed target trajectory and the CE output in white, on a brown background. Grid lines, as included in Fig. 7 for clarification, were not shown. The CE output (circle) was a two-dimensional overlay, so subjects could only distinguish between conditions from the previewed target.

3) Preview Time: The visual preview time τ_p was set to 2 s, well beyond reported critical preview times for integrator CE dynamics [8]–[10].

4) Forcing Functions: The target and disturbance signals' input frequencies were chosen such that an integer number k of their sinusoid periods exactly fitted the measurement time of 120 s. Double bands of input frequencies were used, to allow calculation of the coherence. The bandwidth of both signals was approximately 1.5 rad/s, above which the sinusoids' amplitudes were attenuated 20 dB. The target and disturbance signals standard deviations were 1.27 cm and 0.508 cm, respectively. Five different realizations of the target signal were used during the experiment to prevent subjects from remembering it, after repeated exposure. All forcing function parameters are given in Table I.

C. Apparatus

The experiment was conducted in the fixed-base part-task simulator at TU Delft, Faculty of Aerospace Engineering. Subjects were seated directly in front of the screen on which the display was shown, at a distance of approximately 75 cm. The screen was 36 by 29.5 cm, had a resolution of 1280 by 1024 pixels, and an update rate of 100 Hz. The image generator time delay was in the order of 20-25 ms. To generate control inputs, subjects used an electro-hydraulic servo-controlled side-stick, positioned at their right-hand side. It had a moment arm of 9 cm and could only rotate around its roll axis. The side-stick's torsional stiffness was 3.58 Nm/rad, its torsional damping 0.20 Nm·s/rad, its mass moment of inertia 0.01 kg·m^2, and its gain 0.44 cm/deg.

D. Subjects and Experimental Procedure

The experiment was performed by eight motivated, male volunteers; their tracking experience ranged from novice to experienced. We explained that the experimental goal was to investigate the effect of linear perspective on HC behavior, without giving further information about the individual conditions. Subjects were simply instructed to track the target as well as possible, hence to always minimize the current tracking error $e(t)$. They were informed of their rights and agreed to these by signing a consent form.

The experiment was divided in two sessions of two conditions. Each session took place on a different day to reduce fatigue effects. To get subjects accustomed with the task and the displays, each condition was practiced at least twice before the measurements were started. Then the conditions were presented to the subjects in an order dictated by a balanced Latin-Square design. When stable performance was achieved in a condition, generally after three to eight (128 s long) runs, the five actual measurement runs were recorded, after which subjects moved on to the next condition. On the second day,

TABLE I
FORCING FUNCTIONS PARAMETERS, FIVE TARGET SIGNALS AND ONE DISTURBANCE SIGNAL.

	target signals f_t								disturbance signal f_d			
i, -	k_t, -	A_t, cm	ω_t, rad/s	$\phi_{t,1}$, rad	$\phi_{t,2}$, rad	$\phi_{t,3}$, rad	$\phi_{t,4}$, rad	$\phi_{t,5}$, rad	k_d, -	A_d, cm	ω_d, rad/s	ϕ_d, rad
1	2	0.630	0.105	5.017	5.185	2.676	4.473	4.483	5	0.252	0.262	0.939
2	3	0.630	0.157	4.313	0.570	1.602	1.772	2.604	6	0.252	0.314	2.487
3	8	0.630	0.419	0.000	1.297	3.207	0.721	4.614	11	0.252	0.576	5.016
4	9	0.630	0.471	3.158	4.984	5.360	0.904	4.954	12	0.252	0.628	1.985
5	14	0.630	0.733	6.193	4.283	5.540	1.954	0.557	18	0.252	0.942	1.359
6	15	0.630	0.785	0.044	2.953	4.250	2.709	3.057	19	0.252	0.995	1.105
7	26	0.630	1.361	0.257	5.641	4.175	0.208	4.215	31	0.252	1.623	4.734
8	27	0.630	1.414	0.650	2.567	6.001	5.051	5.770	32	0.252	1.676	1.821
9	40	0.063	2.094	3.791	4.138	2.878	1.891	3.604	58	0.025	3.037	4.937
10	41	0.063	2.147	0.290	6.022	5.151	2.129	3.005	59	0.025	3.089	5.563
11	78	0.063	4.084	2.651	1.896	3.165	0.190	5.865	93	0.025	4.869	4.183
12	79	0.063	4.136	2.236	4.554	6.094	5.892	1.513	94	0.025	4.922	0.350
13	110	0.063	5.760	4.384	4.724	3.065	1.727	2.292	128	0.025	6.702	5.330
14	111	0.063	5.812	2.281	1.166	4.500	1.281	4.865	129	0.025	6.754	4.830
15	148	0.063	7.749	2.039	3.571	0.499	4.448	1.819	158	0.025	8.273	6.123
16	149	0.063	7.802	4.257	0.384	2.712	1.652	1.398	159	0.025	8.325	3.631
17	177	0.063	9.268	3.665	4.293	4.570	5.477	1.165	193	0.025	10.105	5.327
18	178	0.063	9.320	1.511	4.202	2.161	0.959	2.601	194	0.025	10.158	5.996
19	220	0.063	11.519	2.355	0.843	4.464	4.042	2.919	301	0.025	15.760	2.593
20	221	0.063	11.572	1.286	5.611	3.022	1.221	2.209	302	0.025	15.813	3.733

all four conditions were practiced once before the final two conditions were tested.

After each run the subjects were informed of the root-mean-square of their tracking error in that run, to motivate them to optimize their performance. The total experiment lasted about 3.5 hours per subject, approximately evenly distributed over the two sessions. In-between each two conditions a 15 minute break was taken to further reduce fatigue effects.

The time-traces of the error $e(t)$, the CE output $x(t)$, and the operator's control actions $u(t)$ were recorded during the experiment with a sampling frequency of 100 Hz. From the 128 s of each of the recorded time-traces only the last 120 s were used for our analysis; the first 8 s, which contained most of the subjects' transient response, were used as run-in time.

E. Dependent Measures

First, time-traces of the control output were used to compare control behavior between conditions. Second, the variances of the error σ_e^2 and the control output σ_u^2 were used as measures for tracking performance and control activity, respectively. Third, the coherence was used as a measure for the linearity of the subjects' response. Fourth, the nonparametric describing functions were used to compare HC behavior in the frequency domain. Fifth, the describing functions were compared to the model fits to validate the model's ability to describe the measured HC dynamics. Sixth, the VAF was used as a second measure for the model's fitness. Finally, the subjects' control behavior was quantified using the estimated model parameters, the response gains K_n and K_f, and the vertical display coordinate v responded to.

F. Data Processing

The error and control output variances and the coherence were calculated per run. Before applying system identification, all signals were averaged over the five runs in the frequency domain to reduce the remnant contribution in the estimates [26]. Statistics were used to test for significant effects on the error and control output variances, and the model parameters. To reflect within-subject effects only, 95% confidence intervals were calculated after removing between-subject variability, by compensating each subject's data both with that subject's mean over the four condition and the grand mean over all subjects. A repeated-measures two-way ANOVA was used to deal with the experiment's two categorical independent variables: horizontal and vertical display scaling. Each dependent measure was analyzed with a separate test. For some measures, the collected samples in specific conditions were not normally distributed, thereby violating the normality assumption for parametric statistical tests. With no nonparametric equivalent test for a two-way repeated-measured ANOVA, and ANOVAs' known robustness against violations of the normality assumption [32], the ANOVA was still performed.

G. Hypotheses

Due to linear perspective, the previewed target trajectory ahead is horizontally compressed by $K_{d,u}(\tau)$ (see Section II). Considering that the task involves lateral control, HCs can adapt to horizontal perspective by increasing their control gains K_n and K_f. Although ideally the HC inverts the display gains (so the closed-loop dynamics remain equal as in plan-view tasks), subjects in compensatory control tasks increased their control gains insufficiently to compensate for smaller displayed errors, while also increasing their response delay τ_v [18], [19]. Therefore, we hypothesize that:

I: From constant to perspective horizontal scaling, HCs increase their response gains K_n and K_f, but insufficiently

to invert the display gain ($K_{n,eff}$ and $K_{f,eff}$ decrease); HCs also increase their response delay τ_v [18], [19].

Due to linear perspective, the previewed target ahead is also compressed vertically, by $C_{d,v}(\tau)$. Assuming that this vertical compression does not affect perception, we hypothesize that:

II: With and without vertical perspective scaling HC behavior is similar: subjects select the same two viewpoints on the previewed target ahead (characterized by τ_n and τ_f); due to the perspective transformation, however, these correspond to other vertical display coordinates v.

V. Experimental Results

A. Nonparametric Results

1) Control Output: Fig. 8 shows representative time-traces of the measured control outputs. At low frequencies (slow, large amplitude oscillations) the control outputs are similar in all conditions, but at high frequencies (fast, small amplitude oscillations) the control outputs have different amplitudes and are out-of-phase.

2) Performance and Control Activity: Fig. 9 shows the tracking performance and control activity, the corresponding ANOVA results are given in Table II. Overall, task performance is good, considering that the target signal's variance was 1.61 cm^2. The total tracking performance decreases significantly when either horizontal or vertical perspective is added to the plan-view task (NP). However, when horizontal perspective is already present and vertical perspective is added (HP to HVP), performance improves (significant interaction effect). The total control activity is slightly lower when horizontal perspective is present (not significant).

At the disturbance input frequencies (black bars in Fig. 9), both performance and control activity are identical in all conditions (although some differences are significant, see Table II). At the target and remnant frequencies performance drops markedly with horizontal perspective, while control activity decreases at the target frequencies and increases at the remnant frequencies (all significant effects); this suggests that subjects apply a less consistent and less effective control strategy. Similar as for the total performance, vertical perspective has a negative effect on performance at the target and remnant frequencies when added to plan-view tasks (NP to VP), but a positive effect when horizontal perspective is already present (HP to HVP; significant interaction effect).

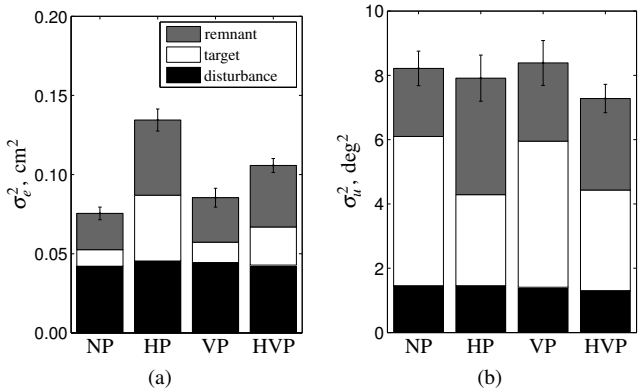

Fig. 9. Variances of the error (a) and the control output (b), mean of all subjects; errorbars indicate 95% confidence intervals.

TABLE II
Error and control output ANOVA results.[1]

			horizontal		vertical		hor.×vert.	
		NV	F	sig.	F	sig.	F	sig.
error, e	total	0	174	**	8.04	*	180	**
	target	1	29.0	**	21.4	**	30.4	**
	disturb.	0	1.04	-	0.01	-	6.28	*
	remnant	1	49.6	**	2.04	-	36.5	**
control output, u	total	2	4.18	-	0.44	-	6.55	*
	target	0	49.0	**	0.40	-	1.97	-
	disturb.	0	2.47	-	21.5	**	11.0	*
	remnant	3	49.0	**	0.40	-	1.97	-

[1] NV is the number of samples that violate the Lilliefors normality test ($p < .05$). Symbols **, *, and - indicate the result is highly significant ($p < .01$), significant ($p < .05$), and not significant ($p > .05$), respectively. Degrees of freedom (df) is always (1,7).

3) Coherence: The average coherence (Fig. 10) between the input signals and the control output is often close to 1, and always above 0.7. The closed-loop human-machine system is thus predominantly linear, even in perspective tasks, which justifies using a quasi-linear model to analyze the experimental data. Especially at frequencies below 2 rad/s the coherence is high. Here, the input signals' amplitudes were large (see Section IV) and well visible, allowing for little observation noise. At higher frequencies, the input signals' amplitudes were 10 times smaller; consequently, more observation noise is present and the coherence drops. With horizontal perspective scaling, the displayed excursions are attenuated even more along the previewed target ahead, yielding a lower coherence

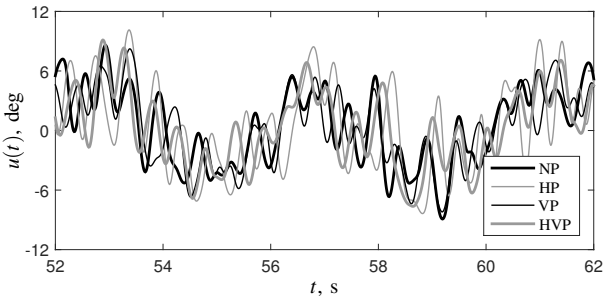

Fig. 8. Measured control outputs for a representative subject, single run data.

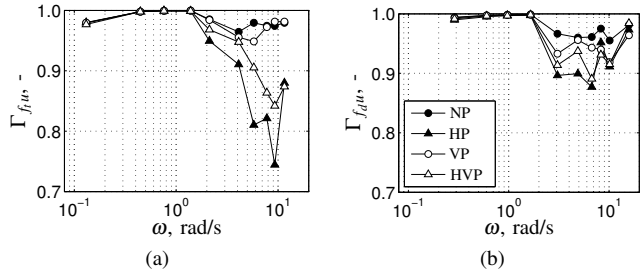

Fig. 10. Coherence between the target (a) and disturbance (b) input forcing functions, and the HC control outputs; mean of all subjects.

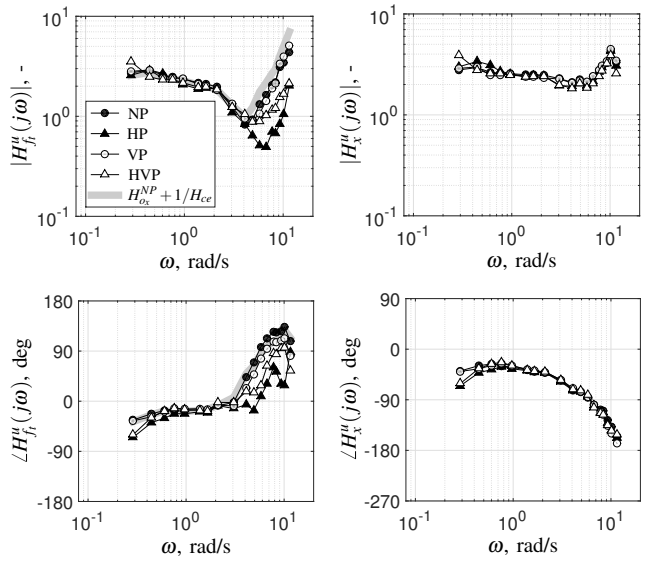

Fig. 11. Nonparametric describing function estimates, mean of all subjects.

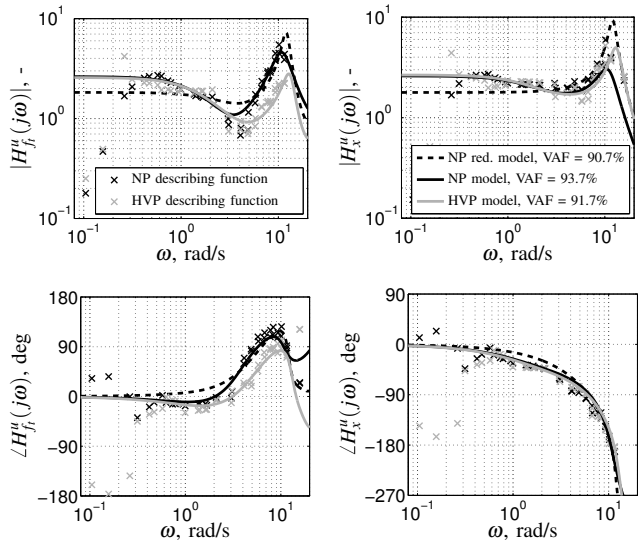

Fig. 12. Estimated describing functions and model fits, single subject data. The reduced model lacks the internal error response lead-lag equalization.

in the HP and HVP conditions. In these conditions where the coherence is low, the remnant is typically large (see Fig. 9b).

4) Describing Functions: Fig. 11 shows the nonparametric describing function estimates. $H_x^u(j\omega)$ is similar in all conditions over the full input frequency range, which indicates that subjects hardly adapted their neuromuscular dynamics, response time delay, and internal-error feedback dynamics, see (14). In plan-view tasks (NP), $H_{f_t}^u(j\omega)$ approximates the dynamics that result in perfect target-tracking (gray line; $H_x^u(j\omega)$ + $1/H_{ce}(j\omega)$, see [12]). Because $H_x^u(j\omega)$ is identical in all conditions (see Fig. 11b and d), the perfect target-tracking dynamics are also similar. With horizontal perspective (HP and HVP) the phase and magnitude required to perfectly track the target signal are matched less well, especially at high frequencies. This corresponds to a lower target-tracking performance in these conditions (see Fig. 9a).

B. Modeling Results

1) Model Fits: Fig. 12 shows both the nonparametric describing function estimates (markers) and the model fits (lines) for a representative subject. The full model fits (including lag-lead equalization) coincide well with the estimated describing functions, which indicates that the model captures most of the subject's control dynamics, also in perspective tasks. A fit with the original model from [11], which lacked lag-lead equalization in integrator tasks (i.e., $H_{o_{e^\star}}(j\omega) = K_{e^\star}$), clearly lacks the capacity to match the describing functions, and has a consistently lower VAF than the full model.

2) Variance Accounted For: For most subjects, the model VAFs (Fig. 13a) are between 80% and 95%, which is higher than in similar manual control modeling attempts [11], [12], [33]. In the HP condition the VAFs are slightly lower, which is in line with the larger remnant (see Fig. 9b). The consistently high VAFs indicate that the model describes all subjects' control behavior well, even in perspective tasks.

3) Model Parameters: Fig. 13 also shows the estimated model parameters, corresponding ANOVA results are given in Table III. The far-viewpoint response gain $K_{f,eff}$ (Fig. 13d) is most consistently affected by linear perspective; this was expected, as perspective deformations are largest far ahead. $K_{f,eff}$ is substantially lower with horizontal perspective (significant effect). The smaller visual stimulus in control direction thus evokes less aggressive control behavior, similar as in compensatory tracking tasks [18], [19]. Vertical perspective results in a higher $K_{f,eff}$, but only when horizontal perspective is already present (HP to HVP; significant interaction effect). Higher values of $K_{f,eff}$ correspond closely to a better tracking performance (see Fig. 9a). Effects of linear perspective on the effective near-viewpoint gain $K_{n,eff}$ (Fig. 13e) are similar to $K_{f,eff}$, but due to larger between-subject variations the statistical results are less pronounced. No systematic adaptation is visible for the near- and far-viewpoint look-ahead times, τ_n and τ_f (Figs. 13h and 13g), nor for the low-pass filter time-constant $T_{l,f}$ (Fig. 13j).

The internal-error response gain $K_{e^\star}$ (Fig. 13f) is slightly lower in all three perspective tasks (compared to NP), but this effect is only significant for vertical scaling. The lead and lag equalization time constants, $T_{L,e^\star}$ and $T_{l,e^\star}$ (Figs. 13b and 13c), are both significantly lower with horizontal perspective. The lag time constant is always about twice as large as lead time constant, reflecting the low-frequency lag-lead equalization visible in Fig. 12. The response time-delay τ_v (Fig. 13i) is slightly, but not significantly, higher in all conditions with perspective scaling, compared to the NP condition, which is similar as in compensatory tracking tasks where the error is displayed smaller [18], [19]. Finally, subjects also adapt the properties of their neuromuscular system, but only to horizontal perspective; here, the neuromuscular break frequency ω_{nms} is significantly higher (Fig. 13k), while the neuromuscular damping ratio ζ_{nms} (Fig. 13l) is significantly lower.

C. Human Controller Adaptation

1) Horizontal Display Direction: The effective gains $K_{n,eff}$ and $K_{f,eff}$ (Figs. 13e and 13d) are lumped combinations of the

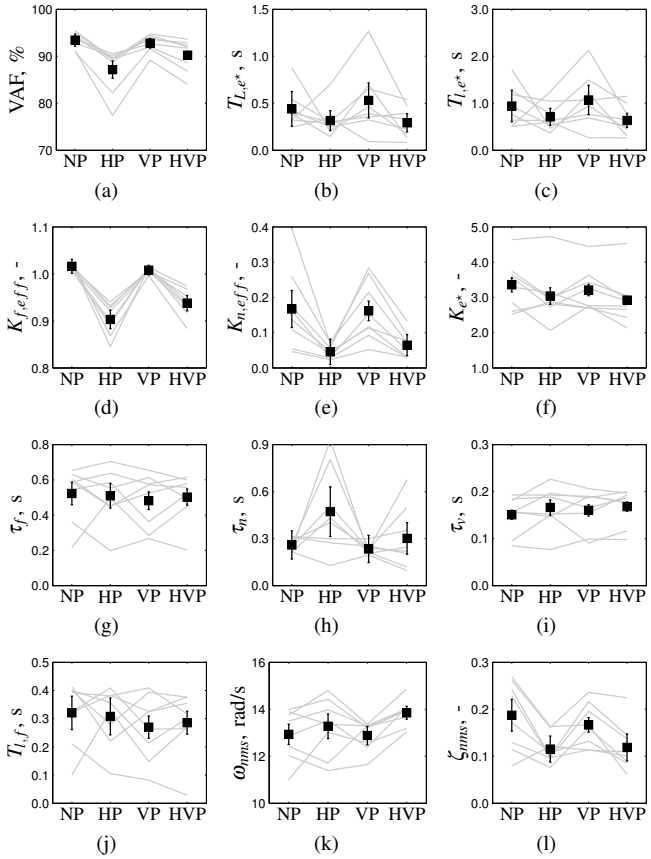

Fig. 13. Estimated model parameters: raw individual subject data (gray lines), and means with 95% confidence intervals corrected for between-subject variability (errorbars).

TABLE III
ESTIMATED PARAMETERS ANOVA RESULTS.[1]

		horizontal		vertical		hor.×vert.	
	NV	F	sig.	F	sig.	F	sig.
$K_{f,eff}$	0	80.7	**	3.77	-	17.6	**
τ_f	1	0.01	-	1.67	-	0.65	-
$T_{l,f}$	1	0.00	-	2.60	-	0.47	-
$K_{n,eff}$	0	17.2	**	0.21	-	1.23	-
τ_n	0	3.54	-	5.54	-	2.93	-
$K_{e^\star}$	2	5.50	-	6.34	*	0.08	-
$T_{L,e^\star}$	1	7.90	*	0.23	-	0.46	-
$T_{l,e^\star}$	0	8.53	*	0.06	-	0.47	-
τ_v	1	3.28	-	0.81	-	0.53	-
ω_{nms}	1	11.2	*	1.26	-	3.04	-
ζ_{nms}	0	15.2	**	0.32	-	1.85	-

[1] NV is the number of samples that violate the Lilliefors normality test ($p < .05$). Symbols **, *, and - indicate the result is highly significant ($p < .01$), significant ($p < .05$), and not significant ($p > .05$), respectively. Degrees of freedom (df) is always (1,7).

HC and the display gains, see (15). To better illustrate HCs' control adaptation to horizontal perspective, Fig. 14 shows the separate contributions of the far-viewpoint gains K_f, $K_{f,eff}$, and $K_{d,u}(\tau_f)$, which are most strongly affected by perspective. HCs more than double their response gain K_f (black markers) to compensate for the reduced display gains (white markers) with horizontal perspective. In other words, subjects respond much more aggressively to the reduced visual stimulus. This

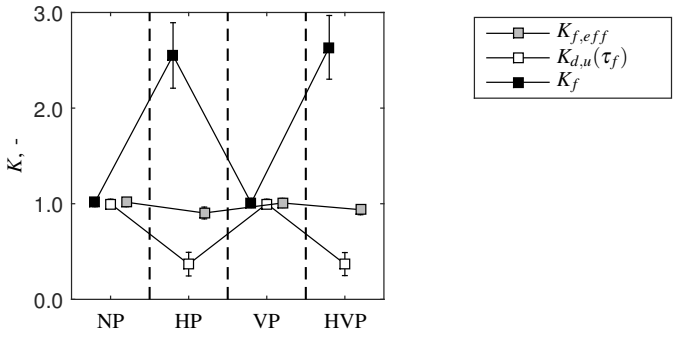

Fig. 14. Estimated far-viewpoint response gain adaptation.

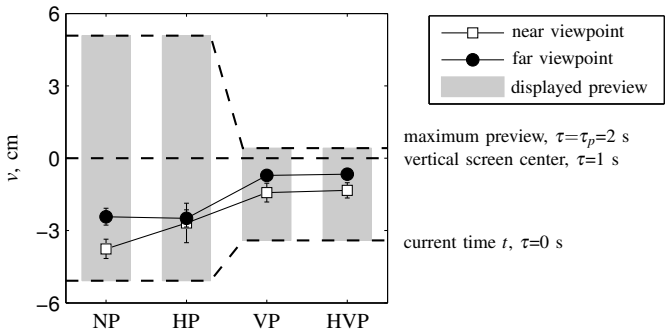

Fig. 15. Vertical location of the near- and far-viewpoints on the display.

adaptation is still less than required to fully invert the display gains, as the combined gain $K_{f,eff}$ is consistently lower with horizontal perspective (HP and HVP conditions). Results for the near-viewpoint gains are similar, see also Fig. 13.

2) Vertical Display Direction: Due to the perspective transformation, the same point on the previewed target ahead corresponds to a different vertical display location in plan-view and perspective conditions. Fig. 15 shows the points on the display that subjects responded to, which clearly illustrates the substantial adaptation required to compensate for vertical perspective deformations. With the introduction of vertical perspective (NP and HP to VP and HVP), subjects shift their near-viewpoint from about 3.5 to 1.5 cm below the screen center, and their far-viewpoint from about 3 to 0.5 cm below the screen center. Moreover, the viewpoints' locations shift from about 25% above the start of the previewed target (at τ=0 s in Fig. 15) to about 25% below the end of the previewed target (at τ=2 s).

VI. DISCUSSION

In the experiment, we measured how linear perspective affects HC use of preview information. With horizontal perspective scaling, we indeed found the hypothesized increase of the response gains K_n and K_f (H.I). Subjects thus responded more aggressively to lower amplitude of the displayed target ahead, but, as expected, not aggressively enough to completely invert the display gain ($K_{n,eff}$ and $K_{f,eff}$ were lower than in the plan-view task). HCs also slightly increased their response time-delay τ_v, confirming H.I. HC adaptation to perspective scaling of a previewed target trajectory appears to be similar

to their adaptation to a reduced scaling of the visual error in compensatory tracking tasks, which also evokes a less aggressive, and more delayed response [18], [19]. Due to the wider variety of HC behavior compared to compensatory tracking, we recommend future preview tracking investigations to test more than the eight subjects used here, to avoid normality violations and improve confidence in the results.

We further hypothesized that vertical perspective scaling would not affect HC behavior (H.II). Indeed, subjects selected approximately the same viewpoints τ_n and τ_f s ahead on the previewed target in conditions with and without vertical perspective, despite their different vertical locations v on the display. However, H.II cannot be fully confirmed, as our results point to a substantial interaction between horizontal and vertical perspective. When vertical perspective is added to a task where horizontal perspective is already present (HP to HVP), subjects reduce their remnant, respond with a higher gain $K_{f,eff}$, and improve their tracking performance. Comparison of the displays in Figs. 7b and 7d yields a possible explanation: the "unnatural" exponential magnification of the approaching previewed target in the HP condition is likely more difficult to anticipate on than the familiar full linear perspective in the HVP condition.

The results in the plan-view condition differ from those in [12], where a similar experiment was performed. Compared to the experiment in [12], our forcing functions contained less high-frequency power, and the displayed signals were magnified horizontally (to keep the target far ahead well visible in perspective conditions). Amongst others, this resulted in a much more aggressive internal error response, as visible from the magnitude of $H_x^u(j\omega)$, which is about two times higher than in [12]. Likely, the higher horizontal display scaling evoked the more aggressive control behavior, which again emphasizes the importance of proper display scaling in manual control tasks. However, future work should also investigate the effects of forcing function characteristics on human control behavior in preview tracking tasks, as these have not been quantified to date.

The model for plan-view preview tracking tasks from [11] accurately described the measured behavior, also in our perspective tasks. For such perspective tasks, it is convenient to lump the linear perspective transformation and the HC dynamics, so the model is mathematically equivalent as for plan-view tasks. Although the lumped model's inputs are no longer the visual stimuli as sensed by the HC, but the actual target and CE output signals before the perspective transformation, the effective gains can be interpreted similar as the HC gains in plan-view tasks.

All subjects were found to apply lag-lead equalization at the lower frequencies, opposed to the pure proportional control strategy often observed in compensatory tracking tasks with integrator CE dynamics [13]. While it was not yet recognized as such, similar lag-lead equalization is visible in the preview tracking results in [11]. Preview information seems to evoke such behavior, which is perhaps best explained as "waiting" (i.e., lagging) for the low-frequency portion of the cognitively calculated, internal error to build up, before more aggressively responding to it. Future investigations into preview tracking tasks with integrator CE dynamics can include the lag-lead equalization in the error response model.

The estimated describing functions showed that HCs use similar control mechanism in perspective and plan-view preview tracking tasks, for perspective transformations that approximate the view on the road during driving or cycling. Unfortunately, several other aspects of HC behavior in such vehicle control tasks are not yet fully understood. For example, the viewing direction generally rotates with the vehicle's attitude. The resulting optical flow can be used by HCs to close an inner feedback-loop [3], [25], which can alleviate the requirements on the outer-loop position control, as tested here. Furthermore, instead of tracking a line, it is generally acceptable to keep a vehicle between two boundaries, like the road's edges. We intend to investigate and model the effects of these elements on HC behavior in our future work.

VII. Conclusion

This paper quantified how linear perspective affects human use of preview information in manual control tasks, using experimental results and both nonparametric and parametric system identification techniques. The compression of the trajectory ahead due to linear perspective evokes less aggressive control behavior and inferior task performance, mainly due to reduced visual stimuli in the control direction (i.e., horizontal perspective scaling). Perspective deformations in the non-controlled (vertical) direction affect human control behavior only marginally. We conclude that humans use preview information similarly in plan-view and perspective tracking tasks. The validity of the previously derived quasi-linear model for preview tracking tasks is extended to perspective tasks, and can thereby be used to design and evaluate man-machine systems in more realistic control tasks.

References

[1] R. A. Hess and A. Modjtahedzadeh, "A preview control model of driver steering behavior," in *Proc. 1989 IEEE Int. Conf. Systems, Man, and Cybernetics*, Cambridge, MA, 1989, pp. 504–509.

[2] S. D. Keen and D. J. Cole, "Bias-free identification of a linear model-predictive steering controller from measured driver steering behavior," *IEEE Trans. Systems, Man, and Cybernetics - Part B: Cybernetics*, vol. 42, no. 2, pp. 434–443, Apr. 2012.

[3] L. Saleh, P. Chevrel, F. Claveau, J. F. Lafay, and M. F., "Shared steering control between a driver and an automation: stability in the presence of driver behavior uncertainty," *IEEE Transactions on Intelligent Transportation Systems*, vol. 14, no. 2, pp. 974–983, Jun. 2013.

[4] R. A. Hess, J. K. Moore, and M. Hubbard, "Modeling the manually controlled bicycle," *IEEE Trans. Systems, Man, and Cybernetics - Part A: Systems and Humans*, vol. 42, no. 3, pp. 545–557, May 2012.

[5] A. J. Grunwald, J. B. Robertson, and J. J. Hatfield, "Experimental evaluation of a perspective tunnel display for three-dimensional helicopter approaches," *Journal of Guidance, Control, and Dynamics*, vol. 4, no. 5, pp. 623–631, Nov.-Dec. 1981.

[6] M. Mulder and J. A. Mulder, "Cybernetic analysis of perspective flight-path display dimensions," *Journal of Guidance, Control, and Dynamics*, vol. 28, no. 3, pp. 398–411, May-Jun. 2005.

[7] T. B. Sheridan, "Three models of preview control," *IEEE Trans. Human Factors in Electronics*, vol. 7, no. 2, pp. 91–102, Jun. 1966.

[8] L. D. Reid and N. H. Drewell, "A pilot model for tracking with preview," in *Proc. 8th Ann. Conf. Manual Control*, Ann Arbor, MI, 1972, pp. 191–204.

[9] M. Tomizuka and D. E. Whitney, "The preview control problem with application to man-machine system analysis," in *Proc. 9th Ann. Conf. Manual Control*, Cambridge, MA, 1973, pp. 429–441.

[10] K. Ito and M. Ito, "Tracking behavior of human operators in preview control systems," *Electrical Eng. in Japan*, vol. 95, no. 1, pp. 120–127, 1975, (Transl.: D.K. Ronbunshi, vol. 95C, no. 2, Feb. 1975, pp 30-36).
[11] K. van der El, D. M. Pool, H. J. Damveld, M. M. van Paassen, and M. Mulder, "An empirical human controller model for preview tracking tasks," *IEEE Trans. on Cybernetics*, vol. 46, no. 11, pp. 2609–2621, Nov. 2016.
[12] K. van der El, D. M. Pool, M. M. van Paassen, and M. Mulder, "Effects of preview on human control behavior in tracking tasks with various controlled elements," *IEEE Trans. on Cybernetics*, 2017, online preprint available.
[13] D. T. McRuer and H. R. Jex, "A review of quasi-linear pilot models," *IEEE Trans. Human Factors in Electronics*, vol. 8, no. 3, pp. 231–249, May 1967.
[14] D. T. McRuer, D. Graham, E. S. Krendel, and W. J. Reisener, "Human pilot dynamics in compensatory systems, theory models and experiments with controlled element and forcing function variations," Air Force Flight Dynamics Laboratory, Wright-Patterson Air Force Base, OH, Tech. Rep. AFFDL-TR-65-15, 1965.
[15] J. J. Gibson, "Visually controlled locomotion and visual orientation in animals," *British Journal of Psychology*, vol. 49, no. 3, pp. 182–194, Aug. 1958.
[16] P. M. T. Zaal, F. M. Nieuwenhuizen, M. M. van Paassen, and M. Mulder, "Modeling human control of self-motion direction with optic flow and vestibular motion," *IEEE Trans. on Cybernetics*, vol. 43, no. 2, pp. 544–556, Apr. 2013.
[17] L. R. Young, "On adaptive manual control," *IEEE Trans. Man-Machine Systems*, vol. 10, no. 4, pp. 292–331, Dec. 1969.
[18] W. H. Levison and R. Warren, "Use of linear perspective scene cues in a simulated height regulation task," in *Proc. 20th Ann. Conf. Manual Control*, Sunnyvale, CA, 1984, pp. 467–490.
[19] S. W. Breur, D. M. Pool, M. M. van Paassen, and M. Mulder, "Effects of displayed error scaling in compensatory roll-axis tracking tasks," in *Proc. AIAA Guidance, Navigation, and Control Conf.*, Toronto, Canada, 2010.
[20] S. Murray, H. Boyaci, and D. Kersten, "The representation of percieved angular size in human primary visual cortex," *Nature Neuroscience*, vol. 9, no. 3, pp. 429–434, Mar. 2006.
[21] W. S. Kim, S. R. Ellis, M. E. Tyler, B. Hannaford, and L. W. Stark, "Quantitative evaluation of perspective and stereoscopic displays in three-axis manual tracking tasks," *IEEE Trans. Systems, Man, and Cybernetics*, vol. 17, no. 1, pp. 61–72, Jan. 1987.
[22] I. D. Haskell and C. D. Wickens, "Two- and three-dimensional displays for aviation: A theoretical and empirical comparison," *The International Journal of Aviation Psychology*, vol. 3, no. 2, pp. 87–109, 1993.
[23] S. Zhai, P. Milgram, and A. Rastogi, "Anisotropic human performance in six degree-of-freedom tracking: An evaluation of three-dimensional display and control interfaces," *IEEE Trans. Systems, Man, and Cybernetics - Part A: Systems and Humans*, vol. 27, no. 4, pp. 518–528, Jul. 1997.
[24] B. T. Sweet, "A model of manual control with perspective scene viewing," in *AIAA Modeling and Simulation Technologies (MST) Conf.*, Boston, MA, 2013.
[25] D. T. McRuer, D. H. Weir, H. R. Jex, R. E. Magdaleno, and R. W. Allen, "Measurement of driver-vehicle multiloop response properties with a single disturbance input," *IEEE Transactions on Systems, Man, and Cybernetics*, vol. 5, no. 5, pp. 490–497, Sep. 1975.
[26] M. M. van Paassen and M. Mulder, "Identification of human operator control behaviour in multiple-loop tracking tasks," in *Proc. 7th IFAC/IFIP/IFORS/IEA Symposium on Analysis, Design and Evaluation of Man-Machine Systems*, Kyoto, Japan, 1998, pp. 515–520.
[27] J. D. Foley, A. van Dam, S. K. Feiner, and J. F. Hughes, *Computer Graphics. Principle and Practice.*, 2nd ed. Reading, MA: Addison-Wesley, 1992.
[28] A. Modjtahedzadeh and R. A. Hess, "A model of driver steering control behavior for use in assessing vehicle handling qualities," *Journal of Dynamic Systems, Measurement, and Control*, vol. 115, no. 3, pp. 456–464, 1993.
[29] D. T. McRuer, R. E. Magdaleno, and G. P. Moore, "A neuromuscular actuation system model," *IEEE Trans. Man-Machine Systems*, vol. 9, no. 3, pp. 61–71, Sep. 1968.
[30] R. L. Stapleford, D. T. McRuer, and R. E. Magdaleno, "Pilot describing function measurements in a multiloop task," *IEEE Trans. Human Factors in Electronics*, vol. 8, no. 2, pp. 113–125, Jun. 1967.
[31] F. C. T. Van der Helm, A. C. Schouten, E. De Vlugt, and G. G. Brouwn, "Identification of intrinsic and reflexive components of human arm dynamics during postural control," *Journal of Neuroscience Methods*, vol. 119, no. 1, pp. 1–14, Sep. 2002.
[32] E. Schmider, M. Ziegler, E. Danay, L. Beyer, and M. Bühner, "Is it really robust? Reinvestigating the robustness of ANOVA against violations of the normal distribution assumption," *Methodology*, vol. 6, no. 4, pp. 147–151, 2010.
[33] F. M. Drop, D. M. Pool, H. J. Damveld, M. M. van Paassen, and M. Mulder, "Identification of the feedforward component in manual control with predictable target signals," *IEEE Trans. Cybernetics*, vol. 43, no. 6, pp. 1936–1949, Dec. 2013.

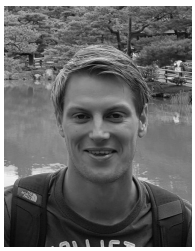

Kasper van der El (S'15) received the M.Sc. degree in aerospace engineering (*cum laude*) from TU Delft, The Netherlands, in 2013, for his research on manual control behavior in preview tracking tasks. He is currently pursuing the Ph.D. degree with the section Control and Simulation, Aerospace Engineering, TU Delft. His Ph.D. research focuses on measuring and modeling human manual control behavior in general control tasks with preview. His current research interests include cybernetics, mathematical modeling, and system identification and parameter estimation.

Daan M. Pool (M'09) received the M.Sc. and Ph.D. degrees (*cum laude*) from TU Delft, The Netherlands, in 2007 and 2012, respectively. His Ph.D. research focused on the development of an objective method for optimization of flight simulator motion cueing fidelity based on measurements of pilot control behavior. He is currently an Assistant Professor with the section Control and Simulation, Aerospace Engineering, TU Delft. His research interests include cybernetics, manual vehicle control, simulator-based training, and mathematical modeling, identification, and optimization techniques.

Marinus (René) M. van Paassen (M'08, SM'15) received the M.Sc. and Ph.D. degrees from TU Delft, The Netherlands, in 1988 and 1994, respectively, for his studies on the role of the neuromuscular system of the pilot's arm in manual control. He is currently an Associate Professor at the section Control and Simulation, Aerospace Engineering, TU Delft, working on human-machine interaction and aircraft simulation. His work on human-machine interaction ranges from studies of perceptual processes and manual control to complex cognitive systems. In the latter field, he applies cognitive systems engineering analysis (abstraction hierarchy and multilevel flow modeling) and ecological interface design to the work domain of vehicle control.

Dr. van Paassen is an Associate Editor of the IEEE TRANSACTIONS ON HUMAN-MACHINE SYSTEMS.

Max Mulder (M'14) received the M.Sc. degree and Ph.D. degree (*cum laude*) in aerospace engineering from TU Delft, The Netherlands, in 1992 and 1999, respectively, for his work on the cybernetics of tunnel-in-the-sky displays. He is currently Full Professor and Head of the section Control and Simulation, Aerospace Engineering, TU Delft. His research interests include cybernetics and its use in modeling human perception and performance, and cognitive systems engineering and its application in the design of "ecological" interfaces.